Inorg. Chem. **2007**, *46*, 4799–4808

Group 4 Transition Metal $CH_2{=}MF_2$, $CHF{=}MF_2$, and $HC{\div}MF_3$ Complexes Formed by C–F Activation and α-Fluorine Transfer

Jonathan T. Lyon and Lester Andrews*

Department of Chemistry, University of Virginia, P.O. Box 400319, Charlottesville, Virginia 22904-4319

Received September 8, 2006

Group 4 transition metal methylidene difluoride complexes ($CH_2{=}MF_2$) are formed by the reaction of methylene fluoride with laser-ablated metal atoms and are isolated in an argon matrix. Isotopic substitution of the CH_2F_2 precursor and theoretical computations (B3LYP and CCSD) confirm product identifications and assignments. Our calculations indicate that the $CH_2{=}MF_2$ complexes have near C_{2v} symmetry and are considerably more stable than other possible products ($CH_2(\mu\text{-F})MF$ and $CHF{=}MHF$). The primary reaction exothermicity provides more than enough energy to activate the initial bridge-bonded $CH_2(\mu\text{-F})MF$ products on the triplet potential energy surface to complete an α-F transfer to form the very stable $CH_2{=}MF_2$ products. Analogous experiments with CHF_3 produce $CHF{=}TiF_2$, which is not distorted at the C–H bond, whereas the heavier group 4 metals form lower-energy triplet $HC{\div}MF_3$ complexes, which contain weak degenerate C(p)–M(d) π-bonding interactions. Comparisons are made with the $CH_2{=}MHF$ methylidene species, which showed considerable agostic distortions.

Introduction

Alkylidene complexes of the form $M{=}CR_1R_2$ are of considerable interest for their role in catalytic processes. Many early transition metal alkylidene complexes are involved as intermediates in a variety of reactions, and they exhibit agostic bonding.[1−4] Hence, investigation of these complexes aids in the understanding of the unique properties of agostic interactions and the process of C−R bond activation. Recently, the study of reactions involving C−F bond activation has emerged as an attractive field,[5−12] but most of this work has focused on aryl−F rather than alkyl−F bonds. Part of the interest in C−F bond activation and hydrodefluorination stems from the need to dispose of chlorofluorocarbons.[8,13−16]

Reactions of group 4 transition metal atoms with CH_4 and CH_3F provide several interesting observations.[17−23] Methyl fluoride is more reactive than methane, and C−F bond activation proceeds exclusively to give $CH_3{-}MF$ as the first product. For both reagents, methylidene complexes are produced by α-H transfer after the formation of the primary

* To whom correspondence should be addressed. E-mail: lsa@virginia.edu.

(1) Buchmeiser, M. R. *Chem. Rev.* **2000**, *100*, 1565.
(2) Schrock, R. R. *Chem. Rev.* **2002**, *102*, 145.
(3) Wada, K.; Pamplin, C. B.; Legzdins, P.; Patrick, B. O.; Tsyba, I.; Bau, R. *J. Am. Chem. Soc.* **2003**, *125*, 7035.
(4) Bailey, B. C.; Fan, H.; Baum, E. W.; Huffman, J. C.; Baik, M.-H.; Mindiola, D. J. *J. Am. Chem. Soc.* **2005**, *127*, 16016.
(5) Kiplinger, J. L.; Richmond, T. G.; Osterberg, C. E. *Chem. Rev.* **1994**, *94*, 373.
(6) Su, M.; Chu, S. *J. Am. Chem. Soc.* **1997**, *119*, 10178.
(7) Chen, Q.; Freiser, B. S. *J. Phys. Chem. A* **1998**, *102*, 3343.
(8) Bosque, R.; Clot, E.; Fantacci, S.; Maseras, F.; Eisenstein, O.; Perutz, R. N.; Renkema, K. B.; Caulton, K. G. *J. Am. Chem. Soc.* **1998**, *120*, 12634.
(9) Jakt, M.; Johannissen, L.; Rzepa, H. S.; Widdowson, D. A.; Wilhelm, R. *J. Chem. Soc., Perkin Trans.* **2002**, 576.
(10) Gerard, H.; Davidson, E. R.; Eisenstein, O. *Mol. Phys.* **2002**, *100*, 533.
(11) Reinhold, M.; McGrady, J. E.; Perutz, R. N. *J. Am. Chem. Soc.* **2004**, *126*, 5268.
(12) Colmenares, F.; Torrens, H. *J. Phys. Chem. A* **2005**, *109*, 10587.
(13) Yang, H.; Gao, H.; Angelici, R. J. *Organometallics* **1999**, *18*, 2285.
(14) Burdeniuc, J.; Jedlicka, B.; Crabtree, R. H. *Chem. Ber./Recl.* **1997**, *130*, 145.
(15) Kraft, B. M.; Lachicotte, R. J.; Jones, W. D. *J. Am. Chem. Soc.* **2001**, *123*, 10973.
(16) Scott, V. J.; Celenligil-Cetin, R.; Ozerov, O. V. *J. Am. Chem. Soc.* **2005**, *127*, 2852.
(17) Andrews, L.; Cho, H.-G.; Wang, X. *Inorg. Chem.* **2005**, *44*, 4834 (Ti + CH_4).
(18) Cho, H.-G.; Wang, X.; Andrews, L. *J. Am. Chem. Soc.* **2005**, *127*, 465 (Zr + CH_4).
(19) Cho, H.-G.; Wang, X.; Andrews, L. *Organometallics* **2005**, *24*, 2854 (Hf + CH_4).
(20) Cho, H.-G.; Andrews, L. *Inorg. Chem.* **2004**, *43*, 5253 (Ti + CH_3F).
(21) Cho, H.-G.; Andrews, L. *J. Phys. Chem. A* **2004**, *108*, 6294 (Ti + CH_3F).
(22) Cho, H.-G.; Andrews, L. *J. Am. Chem. Soc.* **2004**, *126*, 10485 (Zr + CH_3F).
(23) Cho, H.-G.; Andrews, L. *Organometallics* **2004**, *23*, 4357 (Hf + CH_3F).

10.1021/ic061701l CCC: $37.00
Published on Web 12/19/2006

insertion product, and in the CH_3-TiF and $CH_2=TiHF$ pair, α-H transfer is photoreversible.[21] In addition, we find that agostic distortion decreases in the group 4 $CH_2=MHF$ series.[21−23] These simple methylidene complexes provide model compounds for larger analogues with bulky ligands.[1,24] In this study, we react CH_2F_2 and CHF_3 with group 4 metal atoms for comparison. Despite extensive early efforts to theoretically model the group 4 $CH_2=MCl_2$ species,[25−33] we are aware of only one study that computed the $CH_2=TiF_2$ analogue.[29] A preliminary communication on the $CH_2=TiF_2$ complex has been published.[34]

The primary goals of this investigation are 2-fold. First, if we assume that C−F bond activation occurs to form the more stable[22] primary product CH_2F-MF complex, then either α-H or α-F may transfer to the transition metal center. The smaller atomic hydrogen size would make the CHF=MHF complex the kinetic product, whereas the $CH_2=MF_2$ complex would be the more stable thermodynamic product. If only one product forms, it is of interest to probe which process occurs. The second intriguing question is the role of agostic interactions in either possible methylidene complex. Analogous questions apply to the fluoroform case. Group 4 $CH_2=MHF$ complexes possess considerable agostic stabilization,[20−24] and we wish to investigate this possibility for more heavily fluorinated methylidene species.

Experimental and Theoretical Methods

Our experimental setup has been described previously.[35] In this work, Ti, Zr, and Hf metal atoms were produced by ablating a rotating metal target with a pulsed Nd:YAG laser (1064 nm, 10 Hz repetition rate, 10 ns pulse width). Metal atoms were codeposited with 1% CH_2F_2 or isotopic samples (^{13}C, D) and up to 1% CHF_3 diluted in argon onto a cold CsI window at 8 K for a duration of 1 h. Infrared spectra were recorded on a Nicolet Magna 550 spectrometer with a HgCdTe type B detector cooled to 77 K, at 0.5 cm^{-1} resolution. The resulting matrix was subjected to filtered and unfiltered ultraviolet radiation from a medium-pressure mercury arc street lamp (Philips, 175 W, $\lambda > 220$ nm) and annealings to various temperatures, and IR spectra were recorded after each procedure.

Theoretical calculations were first carried out using the Gaussian 98 package[36] and the B3LYP hybrid density functional.[37] The SDD pseudopotential was employed to represent the electronic density of the transition metals, while the 6-311++G(2d,p) basis set was used for all other atoms.[38,39] Geometries were fully relaxed during optimization, and vibrational frequencies were computed analytically. The calculation of vibrational frequencies is not an exact science, particularly for transition metal fluorides, and DFT provides a good approximation. All B3LYP energy values reported include zero-point vibrational corrections. Geometries of select complexes were reoptimized using the more strenuous CCSD method and comparable basis sets (SDD pseudopotential and 6-311++G(2d,-2p) basis).[40] These computationally more expensive calculations were carried out using parallel computing with the NWChem program.[41]

Results and Discussion

Reactions of group 4 metal atoms with CH_2F_2 and CHF_3 will be reported in turn. Infrared spectra include weak absorptions corresponding to $CH_2F_2^+$ (1254.6 and 1245.0 cm^{-1}), CHF_2^+ (1604.8 and 1607.9 cm^{-1}), CHF_2 (1315.5 and 1164.4 cm^{-1}), CF_2 (1220.4 cm^{-1}), and CF (1278.9 cm^{-1}).[42−44]

Ti + CH_2F_2. Atomic titanium reacted with methylene fluoride and produced four new product absorptions at 612.9, 695.4, 705.8, and 740.3 cm^{-1}. All four absorptions increased in intensity after photolysis with a Pyrex filter ($\lambda > 290$ nm) and full arc irradiation ($\lambda > 220$ nm), and they remained nearly unchanged for all annealings (Figure 1). Weak oxide absorptions corresponding to TiO_2 were observed at 917.0 and 946.7 cm^{-1},[45] but no absorption was found in the Ti−H stretching region near 1600 cm^{-1}.[17,21]

The strongest product peak at 740.3 cm^{-1} is near the 740.6 cm^{-1} frequency assigned to the antisymmetric Ti−F stretching mode of TiF_2.[46,47] However, our product absorption shows 0.4 and 1.6 cm^{-1} ^{13}C and D isotopic shifts, respectively,

(24) von Frantzius, G.; Streubel, R.; Brandhorst, K.; Grunenberg, J. *Organometallics* **2006**, *25*, 118.
(25) Rappe, A. K.; Goddard, W. A. III. *J. Am. Chem. Soc.* **1982**, *104*, 297.
(26) Franci, M. M.; Pietro, W. J.; Hout, R. F. Jr.; Hehre, W. J. *Organometallics* **1983**, *2*, 281.
(27) Franci, M. M.; Pietro, W. J.; Hout, R. F. Jr.; Hehre, W. J. *Organometallics* **1983**, *2*, 815.
(28) Gregory, A. R.; Mintz, E. A. *J. Am. Chem. Soc.* **1985**, *107*, 2179.
(29) Dobbs, K. D.; Hehre, W. J. *J. Am. Chem. Soc.* **1986**, *108*, 4663.
(30) Rappe, A. K. *Organometallics* **1987**, *6*, 354.
(31) Cundari, T. R.; Gordon, M. S. *J. Am. Chem. Soc.* **1992**, *114*, 539.
(32) Cundari, T. R.; Klinckman, T. R. *Inorg. Chem.* **1998**, *37*, 5399.
(33) Böhme, U.; Beckhaus, R. *J. Organomet. Chem.* **1999**, *585*, 179.
(34) Lyon, J. T.; Andrews, L. *Organometallics* **2006**, *25*, 1341 (Ti + CH_2F_2).
(35) Andrews, L. *Chem. Soc. Rev.* **2004**, *33*, 123 and references therein.
(36) Frisch, M. J.; Trucks, G. W.; Schlegel, H. B.; Scuseria, G. E.; Robb, M. A.; Cheeseman, J. R.; Zakrzewski, V. G.; Montgomery, J. A., Jr.; Stratmann, R. E.; Burant, J. C.; Dapprich, S.; Millam, J. M.; Daniels, A. D.; Kudin, K. N.; Strain, M. C.; Farkas, O.; Tomasi, J.; Barone, V.; Cossi, M.; Cammi, R.; Mennucci, B.; Pomelli, C.; Adamo, C.; Clifford, S.; Ochterski, J.; Petersson, G. A.; Ayala, P. Y.; Cui, Q.; Morokuma, K.; Rega, N.; Salvador, P.; Dannenberg, J. J.; Malick, D. K.; Rabuck, A. D.; Raghavachari, K.; Foresman, J. B.; Cioslowski, J.; Ortiz, J. V.; Baboul, A. G.; Stefanov, B. B.; Liu, G.; Liashenko, A.; Piskorz, P.; Komaromi, I.; Gomperts, R.; Martin, R. L.; Fox, D. J.; Keith, T.; Al-Laham, M. A.; Peng, C. Y.; Nanayakkara, A.; Challacombe, M.; Gill, P. M. W.; Johnson, B.; Chen, W.; Wong, M. W.; Andres, J. L.; Gonzalez, C.; Head-Gordon, M.; Replogle, E. S.; Pople, J. A. *Gaussian 98*, revision A.11.4; Gaussian, Inc.: Pittsburgh, PA, 2002.
(37) (a) Becke, A. D. *J. Chem. Phys.* **1993**, *98*, 5648. (b) Lee, C.; Yang, Y.; Parr, R. G. *Phys. Rev. B* **1988**, *37*, 785.
(38) Andrae, D.; Haeussermann, U. Dolg, M.; Stoll, H.; Preuss, H. *Theor. Chim. Acta.* **1990**, *77*, 123.
(39) Frisch, M. J.; Pople, J. A.; Binkley, J. S. *J. Chem. Phys.* **1984**, *80*, 3265.
(40) Scuseria, G. E.; Schaefer, H. F., III. *J. Chem. Phys.* **1989**, *90*, 3700 and references therein.
(41) Aprà, E.; Windus, T. L.; Straatsma, T. P.; Bylaska, E. J.; de Jong, W.; Hirata, S.; Valiev, M.; Hackler, M.; Pollack, L.; Kowalski, K.; Harrison, R.; Dupuis, M.; Smith, D. M. A; Nieplocha, J.; Tipparaju V.; Krishnan, M.; Auer, A. A.; Brown, E.; Cisneros, G.; Fann, G.; Früchtl, H.; Garza, J.; Hirao, K.; Kendall, R.; Nichols, J.; Tsemekhman, K.; Wolinski, K.; Anchell, J.; Bernholdt, D.; Borowski, P.; Clark, T.; Clerc, D.; Dachsel, H.; Deegan, M.; Dyall, K.; Elwood, D.; Glendening, E.; Gutowski, M.; Hess, A.; Jaffe, J.; Johnson, B.; Ju, J.; Kobayashi, R.; Kutteh, R.; Lin, Z.; Littlefield, R.; Long, X.; Meng, B.; Nakajima, T.; Niu, S.; Rosing, M.; Sandrone, G.; Stave, M.; Taylor, H.; Thomas, G.; van Lenthe, J.; Wong, A.; Zhang, Z.; *NWChem, A Computational Chemistry Package for Parallel Computers*, version 4.6; Pacific Northwest National Laboratory: Richland, WA, 2004.
(42) Carver, T. G.; Andrews, L. *J. Chem. Phys.* **1969**, *50*, 5100.
(43) Andrews, L.; Prochaska, F. T. *J. Chem. Phys.* **1979**, *70*, 4714 and references therein.
(44) Jacox, M. E.; Milligan, D. E. *J. Chem. Phys.* **1969**, *50*, 3252.
(45) Chertihin, G. V.; Andrews, L. *J. Phys. Chem.* **1995**, *99*, 6356.

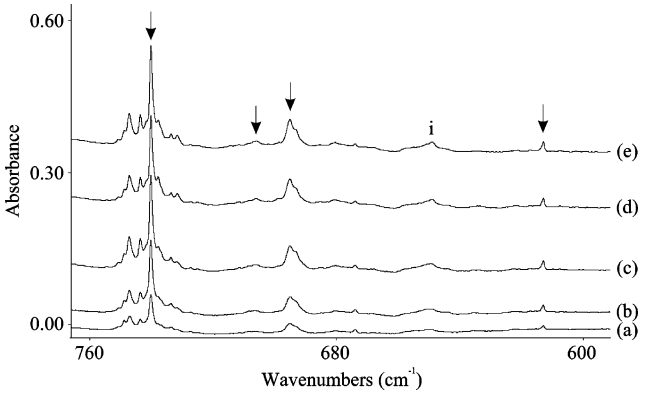

Figure 1. Infrared spectra in the 760−600 cm^{-1} region recorded after (a) laser-ablated titanium atoms were codeposited at 8 K with CH_2F_2 diluted to 1% in argon, and the resulting matrix was subjected to (b) UV radiation of $\lambda > 290$ nm, (c) UV light of $\lambda > 220$ nm, (d) annealing to 30 K, and (e) a final photolysis with $\lambda > 220$ nm.

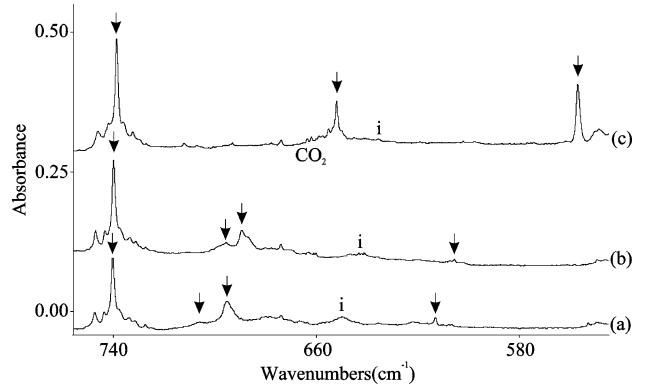

Figure 2. IR spectra taken in the 750−550 cm^{-1} region recorded after titanium atoms were reacted with (a) CH_2F_2, (b) $^{13}CH_2F_2$, and (c) CD_2F_2 at 1% in argon. All spectra were recorded after full arc irradiation.

which indicate that it arises from a complex involving carbon and hydrogen. Since very small carbon and hydrogen isotopic shifts were observed for this particular mode, it can be assigned to a Ti−F stretching motion. The isotopic splittings surrounding this absorption occur from the natural abundance of ^{46}Ti, ^{47}Ti, ^{49}Ti, and ^{50}Ti and are observed at 747.3, 743.7, 737.0 sh, and 733.7 cm^{-1}. Notice that these splittings (3.6, 3.4, 3.3, and 3.3 cm^{-1}) are similar to those observed for the TiF_2 and $(CH_3)_2-TiF_2$ compounds,[20,21,47] demonstrating that our product contains a single titanium atom.

The peak at 705.8 cm^{-1} shows the largest ^{13}C isotopic shift (10.3 cm^{-1}) of the four observed vibrations and a relatively small 54.0 cm^{-1} deuterium shift (Figure 2). These observed isotopic shifts and the region of the spectrum, indicate that this absorption corresponds to a mixed mode involving mostly C═Ti stretching. Notice that the observed ^{13}C isotopic shift is slightly larger than that observed for the CH_2═TiHF complex (9.0 cm^{-1}),[20,21] as B3LYP calculations predict (Table 1).

A strong absorption at 695.4 cm^{-1} reveals the largest deuterium shift of the four observed bands (138.6 cm^{-1}) and

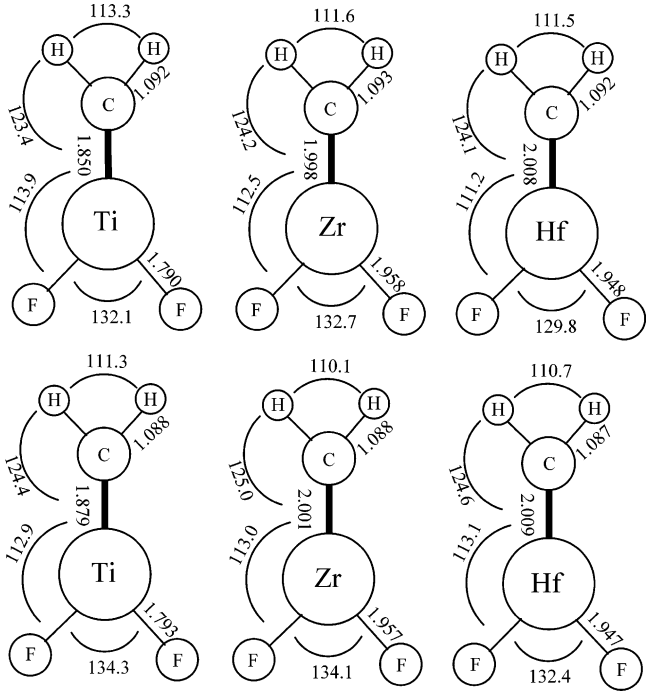

Figure 3. Calculated structures of the CH_2═MF_2 complexes at the B3LYP (top) and CCSD (bottom) levels of theory. All lengths are in angstroms, and angles are in degrees.

a modest 6.0 cm^{-1} carbon-13 shift, and hence, this mode has both carbon and hydrogen character. This region of the spectrum is where we expect a CH_2 wagging motion to appear. The observed frequencies and isotopic shifts are in excellent agreement with those computed for the CH_2═TiF_2 complex (748.2 cm^{-1} frequency and 6.2 and 155.8 cm^{-1} ^{13}C and D isotopic shifts, respectively), leaving little doubt that this observed vibration corresponds to a CH_2 wagging mode.

The final peak observed at 612.9 cm^{-1} shows natural titanium isotopic satellites at 617.2 and 615.3 cm^{-1} for ^{46}Ti and ^{47}Ti, respectively, indicating that this absorption also corresponds to a Ti−F stretching mode. Although the deuterium counterpart of this weaker peak was not observed (the infrared intensity of the deuterium counterpart of the CH_2═TiF_2 complex is computed to be nearly 4 times weaker), the ^{13}C counterpart was observed at 605.4 cm^{-1}. Although this is a larger carbon-13 shift than we would expect for a pure Ti−F stretch, our calculations do predict a larger (4.0 cm^{-1}) carbon-13 isotopic shift for the symmetric Ti−F stretching mode of the CH_2═TiF_2 molecule.

The four observed vibrational modes (Ti−F antisymmetric stretch, Ti−F symmetric stretch, mostly C═Ti stretch, and CH_2 wag) identify the CH_2═TiF_2 complex with confidence. These assignments are confirmed by the general agreement between B3LYP calculated and observed frequencies and isotopic shifts, where the computed values are typically higher by 2−5%[48,49] depending on the molecule and the vibrational mode.[20−23,34] The agreement found for CH_2═TiF_2 is 5.3, 6.6, 7.6, and 5.7% higher harmonic calculated than matrix observed frequencies (740.3, 705.8, 695.4, and 612.9

(46) Hastie, J. W.; Hauge, R. H.; Margrave, J. L. *Chem. Commun.* **1969**, 1452.
(47) Hastie, J. W.; Hauge, R. H.; Margrave, J. L. *J. Chem. Phys.* **1969**, *51*, 2648.
(48) Scott, A. P.; Radom, L. *J. Phys. Chem.* **1996**, *100*, 16502.
(49) Andersson, M. P.; Uvdal, P. *J. Phys. Chem. A* **2005**, *109*, 2937.

Table 1. Observed and Calculated Fundamental Frequencies of $CH_2{=}TiF_2$[a]

approximate mode	$CH_2{=}TiF_2$ obsd	$CH_2{=}TiF_2$ calcd (intensity)	$^{13}CH_2{=}TiF_2$ obsd	$^{13}CH_2{=}TiF_2$ calcd (intensity)	$CD_2{=}TiF_2$ obsd	$CD_2{=}TiF_2$ calcd (intensity)
HCTiF dist., a′		54.1 (59)		53.9 (58)		52.1 (56)
CTiF bend, a″		185.9 (7)		185.0 (4)		154.0 (0)
TiF_2 scis., a′		187.1 (2)		186.0 (5)		184.8 (9)
CH_2 rock, a″		375.5 (1)		370.5 (1)		322.4 (1)
CH_2 twist, a″		519.2 (0)		519.2 (0)		370.3 (0)
Ti−F str., a′	612.9	648.1 (61)	605.4	644.1 (50)		626.1 (16)
CH_2 wag, a′	695.4	748.2 (141)	689.4	742.0 (139)	556.8	592.4 (112)
C═Ti str., a′	705.8	752.7 (95)	695.5	739.1 (103)	651.8	696.8 (118)
Ti−F str., a″	740.3	779.8 (272)	739.9	779.3 (272)	738.7	777.4 (296)
CH_2 scis., a′		1329.3 (18)		1320.0 (17)		1042.6 (31)
CH str., a′		3055.4 (0)		3049.7 (0)		2216.4 (1)
CH str., a″		3145.9 (4)		3133.8 (4)		2334.5 (1)

[a] B3LYP//6-311++G(2d,p)/SDD level of theory. All frequencies are in cm^{-1}, and computed infrared intensities are in km/mol. Mode symmetries for C_s symmetry molecule.

Table 2. Observed and Calculated Fundamental Frequencies of $CH_2{=}ZrF_2$[a]

approximate mode	$CH_2{=}ZrF_2$ obsd	$CH_2{=}ZrF_2$ calcd (intensity)	$^{13}CH_2{=}ZrF_2$ obsd	$^{13}CH_2{=}ZrF_2$ calcd (intensity)	$CD_2{=}ZrF_2$ obsd	$CD_2{=}ZrF_2$ calcd (intensity)
HCZrF dist., a′		60.9 (57)		60.8 (57)		60.4 (54)
ZrF_2 scis., a′		152.6 (6)		151.9 (4)		124.7 (0)
CZrF bend, a″		155.1 (4)		154.4 (5)		152.9 (9)
CH_2 rock, a″		345.4 (3)		340.1 (3)		300.8 (3)
CH_2 twist, a″		529.3 (1)		529.2 (1)		377.3 (0)
Zr−F str., a′	592.1	600.5 (79)	591.5	600.1 (75)	590.9	599.1 (63)
Zr−F str., a″	625.1	646.6 (237)	624.8	646.2 (236)	624.2	644.3 (234)
C═Zr str., a′	676.6	704.1 (61)	659.7	685.6 (63)	608.2	637.5 (66)
CH_2 wag, a′	699.2	758.3 (149)	692.8	751.4 (143)	557.9	596.7 (111)
CH_2 scis., a′		1335.3 (11)		1327.2 (10)		1030.7 (24)
CH str., a′		3045.6 (1)		3039.8 (1)		2210.9 (0)
CH str., a″		3124.7 (7)		3112.9 (8)		2316.5 (2)

[a] B3LYP//6-311++G(2d,p)/SDD level of theory. All frequencies are in cm^{-1}, and computed infrared intensities are in km/mol. Mode symmetries for C_s symmetry molecule.

cm^{-1}, respectively). Similar percentages (6.1, 8.0, 7.0, and 4.2%) were found recently for $CH_2{=}TiHF$.[20,21] Transition metal fluorides are more difficult to model theoretically than compounds with fewer electrons.

In this instance, α-F transfer (rather than α-H transfer) is the dominant process after the initial Ti−F insertion product forms. The computed geometries of this complex at both the B3LYP and CCSD levels of theory are shown in Figure 3. The CCSD geometry is practically identical to the DFT structure, indicating that B3LYP calculations describe these complexes with sufficient accuracy. Notice that the Ti−F bond lengths are only slightly longer than those previously predicted,[29] and that the $CH_2{=}TiF_2$ complex is computed to have no agostic distortion.[34]

A weak absorption at 649.1 cm^{-1} (7.0 and 13.7 cm^{-1} ^{13}C and D shifts, respectively, marked **i** in the figures) also increases upon photolysis and provides evidence for the initial $CH_2(\mu\text{-F})TiF$ primary insertion product. Although there is only one observed vibration for this product, it is in acceptable agreement with the strongest predicted mode of the triplet insertion product (686.7 cm^{-1}; 4.2 and 8.0 cm^{-1} ^{13}C and D isotopic shifts, respectively) which lies 49 kcal/mol higher in energy than the identified $CH_2{=}TiF_2$ complex. Our computations for this insertion product converged to a geometry with one of the fluorine atoms attached to the titanium atom and the other bridging the C−Ti bond. The electron-deficient Ti center prefers this orientation to achieve some overlap with the fluorine electron pairs.

Computations on the possible singlet CHF═TiHF complex converged to a structure 77 kcal/mol higher in energy than the observed $CH_2{=}TiF_2$ product. Although the HC÷$TiHF_2$ complex converged to a stable triplet structure, it is 48 kcal/mol higher in energy than the global minimum-energy singlet $CH_2{=}TiF_2$ complex. Neither of these two higher-energy α-H transfer products was observed here.

Zr + CH_2F_2. The reaction between zirconium atoms and CH_2F_2 gave one major product with absorption peaks at 592.1, 625.1, 676.6, and 699.2 cm^{-1}, which increase together 10−15% upon UV irradiation. Weak impurity absorptions corresponding to ZrO_2 were observed at 817.8 and 884.1 cm^{-1}.[45] The two lower product absorptions at 592.1 and 625.1 cm^{-1} showed small 0.6 and 0.3 cm^{-1} carbon-13 shifts and 1.2 and 0.9 cm^{-1} deuterium shifts, respectively. This is the region expected for Zr−F stretching frequencies because ZrF_2 itself has a strong 633.5 cm^{-1} absorption,[50,51] and these product bands can be assigned to symmetric and antisymmetric Zr−F stretching modes, respectively (Table 2), again on the basis of the general agreement between observed and calculated frequencies.[48,49] Hence, we know that this reaction

(50) Hauge, R. H.; Margrave, J. L. *High Temp. Sci.* **1973**, *5*, 89.
(51) Bukhmarina, V. N.; Dodychin, S. L.; Predtechen, Yu. B.; Shklyarik, V. G. *Zh. Fiz. Khim.* **1986**, *60*, 1775.

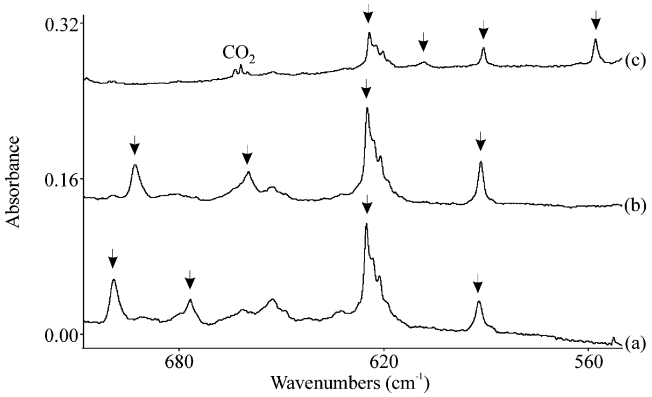

Figure 4. IR spectra taken in the 710−550 cm^{-1} region recorded after zirconium atoms were reacted with (a) CH_2F_2, (b) $^{13}CH_2F_2$, and (c) CD_2F_2 at 1% in argon. All spectra were recorded immediately after deposition.

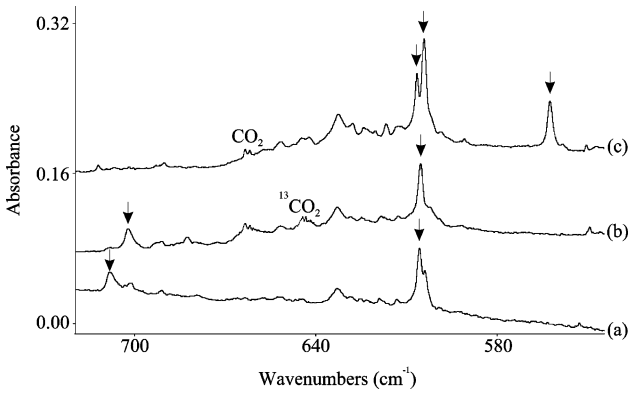

Figure 5. IR spectra taken in the 720−540 cm^{-1} region recorded after hafnium atoms were reacted with (a) CH_2F_2, (b) $^{13}CH_2F_2$, and (c) CD_2F_2 at 1% in argon.

product has two Zr−F bonds. The absorption at 676.6 cm^{-1} shows the largest ^{13}C shift of these four modes (16.9 cm^{-1}) and can be assigned to a mostly C═Zr stretching mode also coupled to the CH_2 bend (Figure 4). The last observed absorption peak at 699.2 cm^{-1} has a 6.4 cm^{-1} carbon-13 shift and a large 141.3 cm^{-1} deuterium shift, which is in satisfactory agreement with our harmonic theoretical prediction (758.3 cm^{-1} with 6.9 cm^{-1} ^{13}C and 161.6 cm^{-1} D isotopic shifts) for the CH_2 wagging motion of the CH_2═ZrF_2 complex. The 1500−1650 cm^{-1} Zr−H stretching region was checked and found to be clear of product absorption.[52] The observation and assignment of these four modes leads to identification of the CH_2═ZrF_2 complex. The agreement between the calculated and observed frequencies (Table 2) is comparable to that described above and found for CH_2═ZrHF.[22]

No other product absorptions were observed in our spectra. Following the titanium considerations, the triplet $CH_2(\mu$-F)-ZrF and singlet CHF═ZrHF complexes were computed by the B3LYP method to be 67 and 76 kcal/mol higher in energy than the singlet CH_2═ZrF_2 molecule, respectively, and the triplet HC÷$ZrHF_2$ complex is 36 kcal/mol higher. The CH_2═ZrF_2 complex is computed at this level to be 166 kcal/mol more stable than the sum of the individual atomic zirconium and CH_2F_2 precursors. The computed geometry of the CH_2═ZrF_2 complex is compared to the titanium analogue in Figure 3 and will be discussed below.

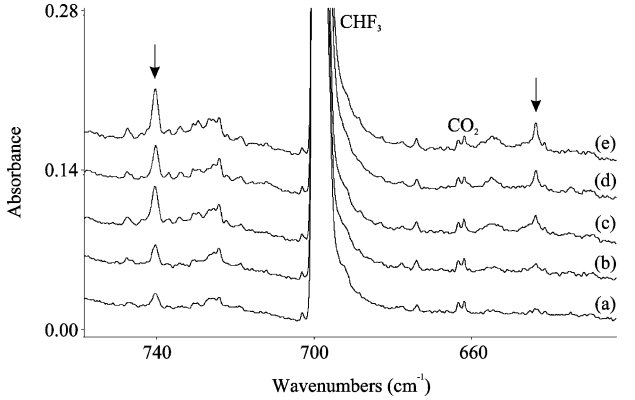

Figure 6. Infrared spectra in the 760−620 cm^{-1} region recorded after (a) laser-ablated titanium atoms were codeposited at 8 K with CHF_3 diluted to 0.25% in argon, and the resulting matrix was subjected to (b) UV radiation of $\lambda > 290$ nm, (c) UV light of $\lambda > 220$ nm, (d) annealing to 30 K, and (e) a final photolysis with $\lambda > 220$ nm.

Hf + CH_2F_2. A single product with new infrared absorptions at 605.6 and 708.3 cm^{-1} was observed from the laser-ablated hafnium reaction with CH_2F_2 in argon (Table 3), and these bands increased slightly together upon UV irradiation. Weak impurity absorptions were observed at 814.0 (HfO_2) and 958.4 (HfO) cm^{-1},[45] and again, the Hf−H stretching region was free of any product absorption.[52] The strongest product peak at 605.6 cm^{-1} shows very small ^{13}C and D isotopic shifts (Figure 5) and is in the correct region for a Hf−F stretching frequency.[23,51] The second absorption at 708.3 cm^{-1} shows a 6.0 cm^{-1} carbon-13 shift and a large 146.0 cm^{-1} deuterium shift and is assigned to the CH_2 wagging motion. The third absorption that is predicted with significant infrared intensity for the anticipated CH_2═HfF_2 complex, the Hf−F symmetric stretch,[3] is not observed in our spectrum. However, our computations predict this absorption to appear very close to the stronger antisymmetric stretch (10 cm^{-1} red-shifted). In the case of the zirconium counterpart, this same theoretical method predicted a 46 cm^{-1} separation between these modes, and a 33 cm^{-1} separation was observed. Hence, we believe that the symmetric Hf−F stretch of the CH_2═HfF_2 complex is hidden underneath the stronger antisymmetric stretching mode. Support for this proposal is found in the CD_2═HfF_2 spectrum where the stronger antisymmetric mode red shifts 1.4 cm^{-1} and reveals a 606.5 cm^{-1} absorption for the symmetric HfF_2 vibration. This mode is slightly blue-shifted by coupling with the CD_2 wagging mode at 562.3 cm^{-1}. Our assignments are validated by comparison with the computed frequencies (Table 3) for the three strongest IR absorptions.

Other possible triplet $CH_2(\mu$-F)HfF, singlet CHF═HfHF, and triplet HC÷$HfHF_2$ complexes were predicted to be 68, 76, and 26 kcal/mol higher in energy than the CH_2═HfF_2 product formed. Finally, the observed CH_2═HfF_2 compound is computed at the B3LYP level to be 162 kcal/mol more stable than the sum of atomic hafnium and methylene fluoride.

Ti + CHF_3. When fluoroform is reacted with titanium, new product absorptions are observed at 643.9 and 740.5

(52) Chertihin, G. V.; Andrews, L. *J. Phys. Chem.* **1995**, *99*, 15004.

Table 3. Observed and Calculated Fundamental Frequencies of $CH_2{=}HfF_2$[a]

approximate mode	$CH_2{=}HfF_2$ obsd	$CH_2{=}HfF_2$ calcd (intensity)	$^{13}CH_2{=}HfF_2$ obsd	$^{13}CH_2{=}HfF_2$ calcd (intensity)	$CD_2{=}HfF_2$ obsd	$CD_2{=}HfF_2$ calcd (intensity)
HCHfF dist., a′		62.6 (41)		62.5 (40)		61.7 (38)
HfF_2 scis., a′		148.1 (8)		147.8 (8)		147.1 (8)
CHfF bend, a″		164.9 (0)		163.2 (0)		137.0 (0)
CH_2 rock, a″		375.2 (4)		370.2 (4)		316.0 (4)
CH_2 twist, a″		519.7 (1)		519.6 (1)		372.7 (0)
Hf−F str., a′	(605)	605.9 (76)	(605)	605.8 (77)	606.5	605.5 (80)
Hf−F str., a″	605.6	616.3 (184)	605.1	615.9 (184)	604.2	613.1 (180)
C=Hf str., a′		696.5 (27)		675.9 (25)		632.0 (10)
CH_2 wag, a′	708.3	754.9 (107)	702.3	748.0 (103)	562.3	594.0 (89)
CH_2 scis., a′		1335.2 (5)		1328.0 (4)		1022.4 (12)
CH str., a′		3059.0 (2)		3053.2 (2)		2220.4 (0)
CH str., a″		3135.4 (5)		3123.6 (6)		2324.5 (1)

[a] B3LYP//6-311++G(2d,p)/SDD level of theory. All frequencies are in cm^{-1}, and computed infrared intensities are in km/mol. Mode symmetries for C_s symmetry molecule.

Table 4. Observed and Calculated Fundamental Frequencies of $CHF{=}TiF_2$[a]

approximate mode	$CHF{=}TiF_2$ obsd	$CHF{=}TiF_2$ calcd (intensity)	$CDF{=}TiF_2$ obsd	$CDF{=}TiF_2$ calcd (intensity)
TiF_2 wag		65.2 (53)		64.8 (52)
FCTiF dist.		97.1 (1)		96.1 (1)
TiF_2 scis.		173.9 (9)		172.9 (9)
FCH rock		243.7 (5)		219.3 (2)
TiCH bend		259.9 (3)		255.1 (2)
C=Ti str.		550.5 (5)		514.5 (5)
Ti−F str.	643.9	680.0 (157)	643.2	676.4 (149)
CH wag	*b*	701.2 (98)	539.5	565.4 (77)
Ti−F str.	740.5	777.0 (261)	739.4	776.4 (265)
C−F str.	*b*	1136.5 (196)	*b*	1199.4 (196)
FCH bend		1334.4 (22)		976.2 (56)
C−H str.		2998.5 (19)		2201.8 (11)

[a] B3LYP//6-311++G(2d,p)/SDD level of theory. All frequencies are in cm^{-1}, and computed infrared intensities are in km/mol. [b] Region covered by intense precursor absorption.

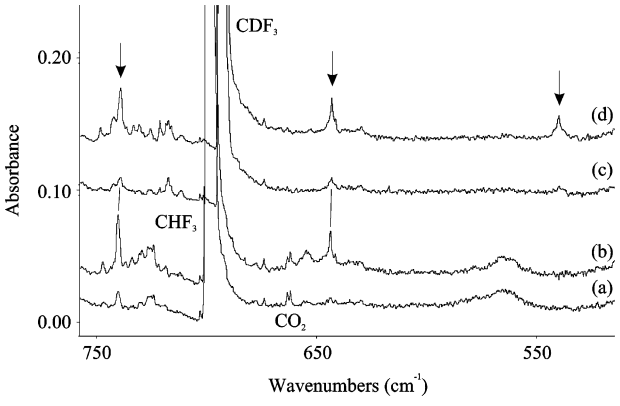

Figure 7. Infrared spectra taken in the 750−520 cm^{-1} region after (a) laser ablated titanium atoms were reacted with dilute CHF_3 in argon and (b) the resulting matrix was subjected to UV radiation of $\lambda > 220$ nm and (c) after laser ablated Ti was reacted with CDF_3 in argon and (d) the resulting matrix was subjected to UV radiation of $\lambda > 220$ nm.

cm^{-1}. Both bands show the same behavior, increasing upon UV photolysis and decreasing slightly upon annealing (Figure 6), and can be assigned to a single reaction product. The first peak shifts to 643.2 cm^{-1} when CDF_3 was employed (Table 4): this very small deuterium shift identifies a Ti−F stretching mode. The second absorption shows only a slightly larger deuterium shift to 739.4 cm^{-1} and must also be

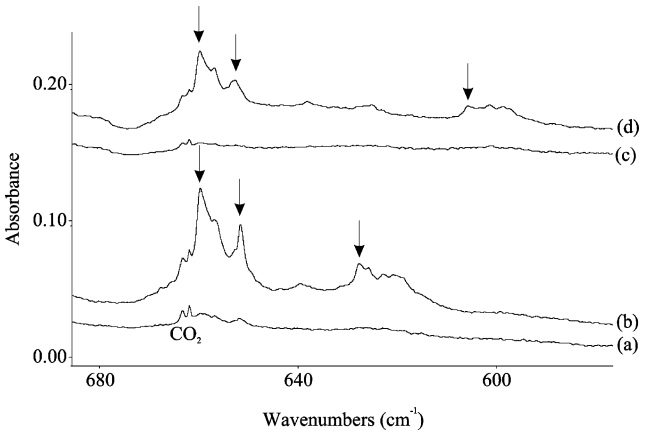

Figure 8. Infrared spectra taken in the 680−580 cm^{-1} region after (a) laser ablated zirconium atoms were reacted with dilute CHF_3 in argon and (b) the resulting matrix was subjected to UV radiation of $\lambda > 220$ nm and (c) after laser ablated Zr was reacted with CDF_3 in argon and (d) the resulting matrix was subjected to UV radiation of $\lambda > 220$ nm.

Table 5. Observed and Calculated Fundamental Frequencies of $HC{\div}ZrF_3$[a]

approximate mode/symmetry	$HC{\div}ZrF_3$ obsd	$HC{\div}ZrF_3$ calcd (intensity)	$DC{\div}ZrF_3$ obsd	$DC{\div}ZrF_3$ calcd (intensity)
FZrC bend, e		162.8 (5)		151.9(7)
FZrF bend, e		164.3 (22)		165.6 (17)
ZrF_3 umbrella, a_1		175.0 (22)		174.2 (23)
Zr−C−H bend, e		426.2 (76)		332.0 (52)
C−Zr str., a_1	627.6	631.1 (13)	605.8	611.1 (58)
Zr−F str., a_1	651.7	643.5 (176)	652.4	641.3 (126)
Zr−F str., e	659.7	660.7 (388)	659.7	660.6 (382)
C−H str., a_1		3169.5 (4)		2336.3 (9)

[a] B3LYP//6-311++G(2d,p)/SDD level of theory. All frequencies are in cm^{-1}, and computed infrared intensities are in km/mol. Mode symmetries for C_{3v} symmetry molecule.

assigned to a Ti−F stretch. In addition, when experiments were performed with CDF_3, a third absorption was observed at 539.5 cm^{-1} with the same photolysis behavior as the other two absorptions (Figure 7).

Three potential products need to be considered for assignment to the observed vibrations. The first is the triplet primary insertion CHF(μ-F)TiF product, which is computed to be 78 kcal/mol more stable than the sum of the titanium atom and CHF_3 precursors. However, two Ti−F stretching

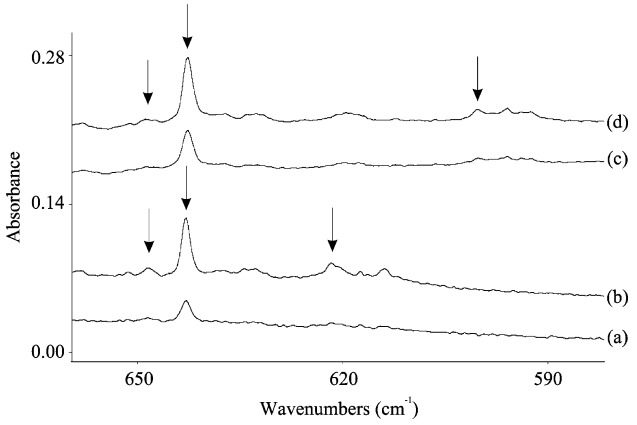

Figure 9. Infrared spectra taken in the 660−580 cm^{-1} region after (a) laser ablated hafnium atoms were reacted with dilute CHF_3 in argon and (b) the resulting matrix was subjected to UV radiation of $\lambda > 220$ nm and (c) after laser ablated Hf was reacted with CDF_3 in argon and (d) the resulting matrix was subjected to UV radiation of $\lambda > 220$ nm.

Table 6. Observed and Calculated Fundamental Frequencies of HC÷HfF_3[a]

	HC÷HfF_3		DC÷HfF_3	
approximate mode/symmetry	obsd	calcd (intensity)	obsd	calcd (intensity)
FHfF bend, e		156.9 (21)		149.8 (11)
HfF_3 umbrella, a_1		160.8 (23)		160.5 (24)
FHfC bend, e		168.7 (5)		165.8 (12)
Hf−C−H bend, e		427.8 (74)		332.2 (50)
C−Hf str., a_1	621.7	618.7 (126)	600.3	596.9 (96)
Hf−F str., e	642.9	630.0 (291)	642.7	629.9 (290)
Hf−F str., a_1	648.6	638.3 (18)	648.6	636.7 (43)
C−H str., a_1		3185.8 (3)		2348.6 (9)

[a] B3LYP//6-311++G(2d,p)/SDD level of theory. All frequencies are in cm^{-1}, and computed infrared intensities are in km/mol. Mode symmetries for C_{3v} symmetry molecule.

frequencies were observed, which rules out this possible product. Next, α-F transfer creates the singlet CHF═TiF_2 complex, which is predicted to be 44 kcal/mol more stable than the primary insertion product. Our computations for this complex predicted four strong absorptions at 680.0, 701.2, 777.0, and 1136.5 cm^{-1} (Table 4). The two Ti−F stretching modes match our observed peaks, but the other two strong absorbers are in regions covered by CHF_3 precursor absorptions. The third vibration observed in the deuterated experiment (539.5 cm^{-1}) is in agreement with the predictions for the DCF wagging mode in CDF═TiF_2, which fortunately is not covered by precursor. Hence the observed vibrations can be assigned to the CHF═TiF_2 complex, analogous to CH_2═TiF_2 discussed above. The third possible reaction product that needs to be considered is triplet HC÷TiF_3. Although this complex is predicted to be 21 kcal/mol more stable than singlet CHF═TiF_2, the computed infrared spectrum (two strong absorptions at 738.7 and 779.9 cm^{-1}) does not reproduce the observed spectrum. In particular, three absorptions were observed when Ti was reacted with CDF_3, but only two observable bands are predicted for DC÷TiF_3. We find an energy barrier to the formation of this triplet HC÷TiF_3 complex (see the Reaction Mechanisms section).

Zr + CHF_3. Zirconium atoms react with CHF_3 to produce a single product with infrared absorptions at 659.7, 651.7, and 627.6 cm^{-1} (Figure 8), which track together upon irradiation just as the new bands in Figure 6. The upper two absorptions do not show substantial isotopic shifts, indicating that they arise from Zr−F stretching modes. However, the lower absorption at 627.6 cm^{-1} red shifts nearly 22 cm^{-1} upon D isotopic substitution suggesting a mode with slight coupling to H and D, such as a carbon-zirconium stretching frequency (see Table 5).

Considering the same three possible products as in the titanium experiments, we computed the CHF(μ-F)ZrF complex to be 89 kcal/mol lower in energy than the sum of the initial reactants. Again, the two Zr−F stretching modes eliminates this complex as the observed product. The singlet CHF═ZrF_2 methylidene complex is 60 kcal/mol more stable than the primary insertion product. For this species, the two Zr−F stretching frequencies are computed to be 646.0 and 605.0 cm^{-1}, which are lower than the observed bands and make the CHF═ZrF_2 complex an unlikely assignment. The third possible product is the triplet HC÷ZrF_3 complex, which is computed to be 38 kcal/mol more stable than the methylidene and to have essentially C_{3v} symmetry. The two Zr−F stretching modes are predicted at 660.7 and 643.5 cm^{-1}, which are in good agreement with observed values. For this complex, the weak Zr−C stretching mode is

Table 7. Geometrical Parameters and Physical Constants of Ground State CH_2═MF_2 (M = Ti, Zr, Hf)[a]

parameter	CH_2═TiF_2	CH_2═ZrF_2	CH_2═HfF_2
r(C−H)	1.092	1.093	1.092
r(C═M)	1.850	1.998	2.008
r(M−F)	1.790	1.958	1.948
∠(HCH)	113.3	111.6	111.5
∠(CMF)	113.9	112.5	111.2
∠(FMF)	132.1	132.7	129.8
∠(HCM)	123.4	124.2	124.1
Φ(HCMF)	1.4, 177.5	5.6, 170.4	9.6, 162.1
q(C)[b]	−0.63/−0.88	−0.93/−1.13	−0.75/−1.23
q(H)[b]	0.13/0.19	0.11/0.20	0.12/0.21
q(M)[b]	1.20/1.71	1.63/2.13	1.35/2.24
q(F)[b]	−0.41/−0.60	−0.46/−0.70	−0.41/−0.71
μ[c]	0.52	1.31	2.37
ΔE[d]	137	166	162

[a] Bond lengths and angles are in Å and deg, respectively. All calculations performed at the B3LYP//6-311++G(2d,p)/SDD level. [b] Mulliken/Natural atomic charges. [c] Molecular dipole moment in D. [d] Binding energy in kcal/mol.

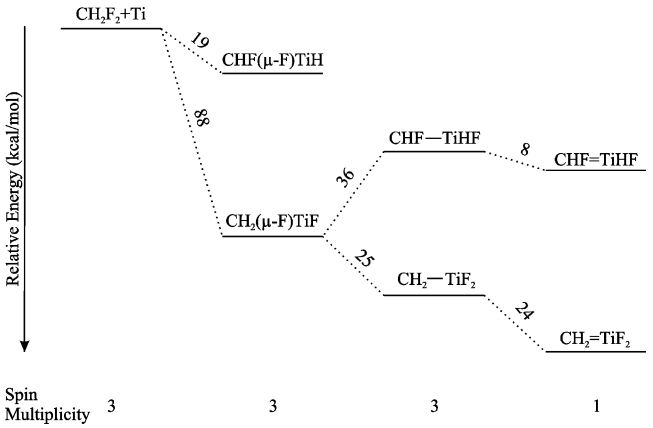

Figure 10. Relative energies of possible titanium and CH_2F_2 products and intermediates calculated at the B3LYP//6-311++G(2d,p)/SDD level of theory. All energy values are in kcal/mol.

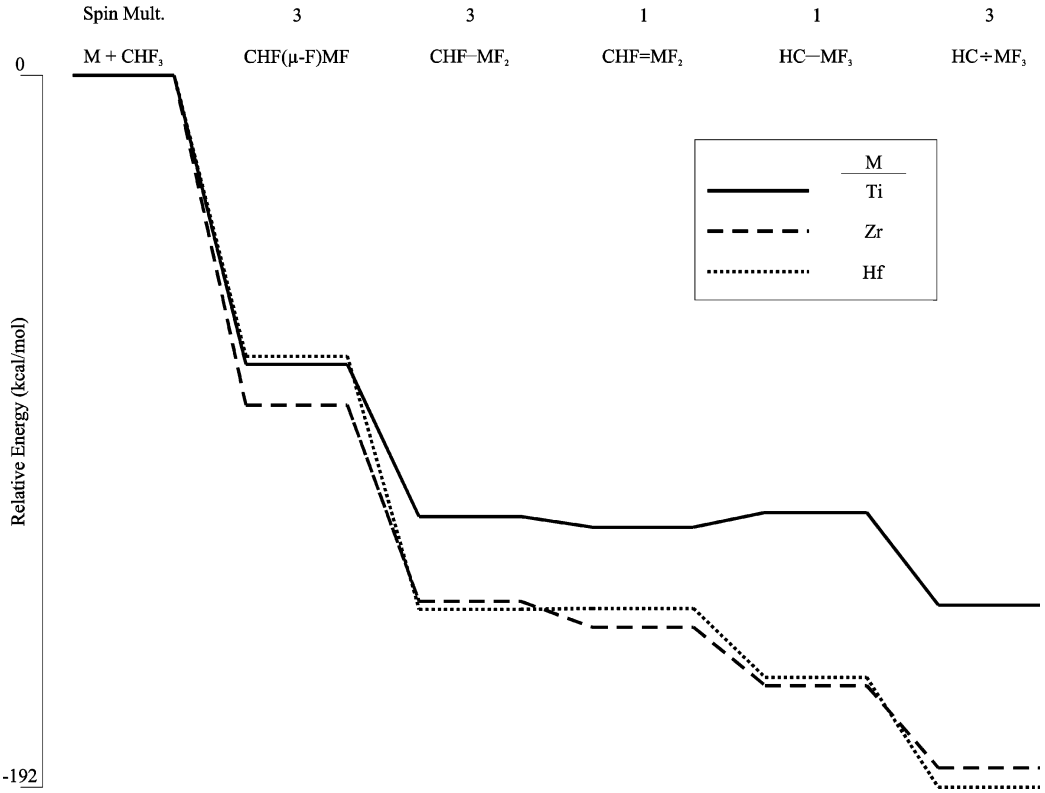

Figure 11. Relative energies of possible group 4 transition metal atom and CHF_3 reaction products and intermediates calculated at the B3LYP//6-311++G-(2d,p)/SDD level of theory. All energy values are in kcal/mol.

computed at 631.1 cm^{-1} with a 20.0 cm^{-1} deuterium shift. This matches our experimental values (Table 5) considerably better than the methylidene product and warrants assignment of the observed product absorptions to the triplet $HC{\div}ZrF_3$ species.

Hf + CHF_3. Absorption peaks are observed at 648.6, 642.9, and 621.7 cm^{-1} when laser-ablated hafnium atoms were reacted with fluoroform. All three absorptions increase in concert upon UV irradiation, decrease slightly upon annealing, and can be assigned to a common product. When deuterated trifluoromethane was employed in experiments, these absorptions shifted to 648.6, 642.7, and 600.3 cm^{-1} (Figure 9). The observed isotopic shifts are in accord with assigning these peaks to two Hf−F and one C−Hf band stretching modes.

The CHF(μ-F)HfF complex was calculated to be 84 kcal/mol more stable than the individual Hf atom and CHF_3 combined, whereas the $CHF{=}HfF_2$ methylidene is 60 kcal/mol more stable than this primary insertion complex. This species is computed to have Hf−F stretching modes at 617.2 and 611.9 cm^{-1}, which is more than 30 cm^{-1} lower than the observed values. In addition, the C═Hf stretching mode is predicted at 521.3 cm^{-1} with a 38.0 cm^{-1} deuterium red shift. This is more than 100 cm^{-1} lower than the experimental C−Hf stretching mode, and the isotopic shift is 16.6 cm^{-1} more than observed. Hence, the reaction product is not this $CHF{=}HfF_2$ methylidene. The third product that needs to be considered is the triplet $HC{\div}HfF_3$ complex with C_{3v} symmetry, which is predicted to be 192 kcal/mol lower in energy than the combined reagents. In this instance, the two Hf−F stretches are computed at 638.3 and 630.0 cm^{-1} in better agreement with experiment (Table 6). The Hf−C stretching mode is predicted at 618.7 cm^{-1} with a 21.8 cm^{-1} deuterium shift, which reproduces the observed values (621.7 cm^{-1} and 21.4 cm^{-1} D shift) extremely well. Therefore, we identify the new product as the $HC{\div}HfF_3$ complex.

Group Trends, Reaction Mechanisms, and Bonding Considerations. The computed $CH_2{=}MF_2$ structures are shown in Figure 3 and parameters are listed in Table 7. Although the geometries optimized without constraints to a near C_{2v} structure (hence we give only one bond length and angle for each set), very small deviations were observed in the planarity of the complexes. At the B3LYP level, the H−C−M−F dihedral angles deviate more from 180°/0° as the metal atom is changed going down the transition series (Table 7). The sum of the three angles around the metal center also decreases in this same order, and the fluorine atoms attached to the metal atom move slightly out of the plane of the other four atoms. Our results from CCSD calculations predict this same behavior but to a lesser extent. As this distortion is small, we performed a check and reoptimized the $CH_2{=}HfF_2$ complex (which is predicted to show the largest distortion) confined in C_{2v} symmetry at the B3LYP level, and this structure produced one imaginary frequency (−63.1 cm^{-1}) for the out-of-plane Hf−F_2 motion.

In the reaction between titanium atoms and CH_2F_2, possible reaction pathways are shown in Figure 10. The primary C−F activation product formed from the insertion of titanium atoms into a C−F bond lies 88 kcal/mol lower in energy than the reactant precursors (and 69 kcal/mol lower in energy than the possible C−H activated CHF(μ-F)TiH insertion complex). Next either an α-hydrogen or α-fluorine

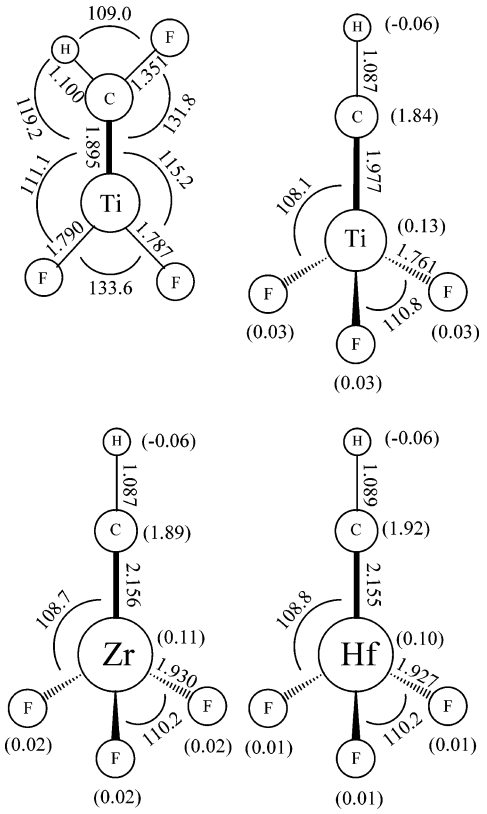

Figure 12. Calculated structures at the B3LYP//6-311++G(2d,p)/SDD level of theory for the major products from group 4 transition metal atom reactions with CHF_3. All bond lengths are in angstroms, and the angles are in degrees. Mulliken atomic spin densities are given parenthetically for triplet complexes.

atom can transfer to the metal center (with the triplet spin multiplicity conserved). However, the triplet CH_2-TiF_2 complex is computed to be 61 kcal/mol lower in energy than triplet CHF−TiHF. The excited CH_2-TiF_2 complex relaxes to the singlet $CH_2{=}TiF_2$ methylidene, which is 24 kcal/mol more stable.

Several comparisons within this series of methylidene complexes are of interest: consider first, $CH_2{=}$TiHF, $CH_2{=}TiF_2$, and $CHF{=}TiF_2$. The computed Ti−F distances are nearly the same (1.786 to 1.790 Å), and the stretching frequencies follow this trend in the region from 757.8 ($CH_2{=}$TiHF) to 612.9 cm^{-1} (symmetric mode for $CH_2{=}TiF_2$). The computed C=Ti distances (1.812, 1.850, and 1.895 Å, respectively) show the inductive effect of more fluorine to weaken the C=Ti bond, and the C=Ti stretching mode, although mixed with motions involving hydrogen, decreases in the series. The CH_2 wagging mode increases from 652.8 cm^{-1} for $CH_2{=}$TiHF to 695.4 cm^{-1} for $CH_2{=}TiF_2$, and although the C−H wagging mode for $CHF{=}TiF_2$ is masked by CHF_3, the C−D wagging mode for $CDF{=}TiF_2$ (539.5 cm^{-1}) falls between the CD_2 wagging modes for the former complexes. The wagging motion is considerably anharmonic because the H/D ratios are 1.250 and 1.249, respectively, for the former two complexes, which may be compared to the 1.318 ratio for the analogous out-of-plane motion for $CH_2{=}CH_2/CD_2{=}CD_2$.[53]

Table 8. Geometrical Parameters and Physical Constants of Ground State $HC{\div}MF_3$ (M = Ti, Zr, Hf)[a]

parameter	$HC{\div}TiF_3$	$HC{\div}ZrF_3$	$HC{\div}HfF_3$
r(C−H)	1.087	1.087	1.089
r(C=M)	1.977	2.156	2.155
r(M−F)	1.761	1.930	1.927
∠(CMF)	108.1	108.7	108.8
∠(FMF)	110.8	110.2	110.2
q(C)[b]	−0.49	−0.84	−0.52
q(H)[b]	0.16	0.10	0.17
q(M)[b]	1.30	1.92	1.46
q(F)[b]	−0.33	−0.39	−0.37
μ[c]	2.37	2.09	1.99
ΔE[d]	143	187	192

[a] Bond lengths and angles are in Å and deg, respectively. All calculations performed at the B3LYP//6-311++G(2d,p)/SDD level. [b] Mulliken atomic charges. [c] Molecular dipole moment in D. [d] Binding energy in kcal/mol.

In the group 4 $CH_2{=}MF_2$ series, the CH_2 wagging modes increase slightly as the molecular framework becomes more rigid, and the anharmonicities decrease slightly as the H/D frequency ratios increase in the series (1.249, 1.253, and 1.260, respectively) Of course, the $M-F_2$ frequencies decrease in the series as summarized in Tables 1−3.

The addition of the second fluorine atom prevents agostic interaction and distortion even though strong interactions were observed in the $CH_2{=}MH_2$ and $CH_2{=}$MHF complexes.[17−23] Agostic stabilization can be thought of as a positively charged metal center attracting the bonded electrons of an adjacent atom (i.e., the C−H-bonded electrons in this molecule). The $CH_2{=}$TiHF complex, where the Ti Mulliken charge is computed to be 0.89,[21] shows considerable agostic distortion. In the present case, the second fluorine atom pulls more electron density away from the titanium center, leaving Ti with a larger 1.20 Mulliken charge, and this should encourage agostic bonding to an even greater extent. A similar increase in charge is found for the Zr and Hf centers (compare Table 4 and Table 2 in ref 23). In the monofluorine analogs, the agostic hydrogen is trans to the fluorine atom.[20−23] The cis form of $CH_2{=}$TiHF is computed to be 3 kcal/mol higher in energy than the trans structure, which is on the order of an agostic bonding interaction.[24] Hence, we conclude that repulsion from the fluorine lone-pair electrons is substantial enough to prevent the agostic interaction in these $CH_2{=}MF_2$ complexes that is clearly observed in the $CH_2{=}$MHF counterparts.[23] The longer C=M bond in the difluoride complex presumably caused by the added inductive effect of a second fluorine mitigates against rearrangement to stabilize the C=M bond.

The energies of the reaction pathways for fluoroform are diagramed in Figure 11. First, the metal atom inserts into a C−F bond forming the CHF(μ-F)MF complexes. Then, with the triplet-spin multiplicity conserved, α-F transfer occurs, and the $CHF-MF_2$ complexes are formed. These species then relax to the singlet-state $CHF{=}MF_2$ complexes. Up to this point, the process has been spontaneous and exothermic along all three metal atom reaction pathways. From here, another fluorine atom transfers to the metal atom, while the singlet

(53) Herzberg, G. *Infrared and Raman Spectra*; Van Nostrand: Princeton, NJ, 1945.

multiplicity is conserved. This step is 16 and 19 kcal/mol exothermic for the zirconium and hafnium complexes, respectively, *but* it is 4 kcal/mol endothermic for the titanium analogue. Irradiation could in principle surmount this small barrier, but excited states required for this photochemical rearrangement are not activated in this system. Hence, the reaction stops along the titanium pathway at the $CHF{=}TiF_2$ complex, whereas the other two metals form lower-energy singlet $HC{-}MF_3$ complexes which relax to even lower energy triplet-state $HC{\div}MF_3$ complexes. The triplet state is lower energetically than the singlet state (22 and 30 kcal/mol, respectively) because each of the unpaired electrons on carbon resides in π orbitals and are partially shared with the electron-deficient metal atom.

The carbon−metal bond in the $HC{\div}MF_3$ complexes includes partially occupied degenerate π_x and π_y molecular orbitals. The computed structures are shown in Figure 12, and the parameters are given in Table 8. The C−Zr and C−Hf bonds are shorter than the single-bonded singlet-state analog (0.009 and 0.028 Å, respectively), but they are longer than computed for the singlet methylidene complexes ($CHF{=}MF_2$) (0.127 and 0.115 Å, respectively), indicating some donation of the unpaired electron density to the metal centers. The NBO analysis[36] shows that these π orbitals each contain 0.998 α-spin electron, and each π orbital is 85.8% C(2p) and 14.2% Zr (4d) or 87.9% C(2p) and 12.1% Hf(5d), which is consistent with a weak π-bonding interaction.[54] This is verified by the 0.11 and 0.10 spin densities on Zr and Hf at the expense of carbon.

Although the $HC{\div}TiF_3$ complex was not observed for kinetic reasons, the computed singlet complex C−Ti bond (2.026 Å) is 0.049 Å longer than that for the triplet complex (1.977 Å). This suggests more π (p−d) bonding for Ti than for Zr and Hf because of more favorable p−d overlap. The spin densities given in Figure 12 support this conclusion. A stronger p−d π-bonding interaction has been observed for the related triplet $FC{\div}TiF_3$ complex.[55]

Conclusions

Group 4 transition metals react with methylene fluoride to yield the $CH_2{=}MF_2$ complex as the primary product trapped in solid argon. Isotopic substitution of the CH_2F_2 precursor and comparison with frequency calculations and isotopic shifts confirm the identified products. For all three transition metals, α-fluorine transfer occurs after the initial $CH_2(\mu\text{-}F)MF$ insertion product is formed. The B3LYP and CCSD computations predict nearly identical structures, which indicate that DFT computations are adequate for computing the properties of these and similar complexes. All three $CH_2{=}MF_2$ methylidene complexes were computed to have near C_{2v} symmetry. Agostic distortions were not observed in these structures in part because of the repulsions between fluorine electron lone pairs and the C−H-bonding electrons. Reactions with CHF_3 form an analogous singlet methylidene $CHF{=}TiF_2$ with titanium, but zirconium and hafnium are able to produce lower-energy triplet $HC{\div}MF_3$ species. These triplet complexes exhibit weak C(p)−M(d) π-bonding interactions.

Acknowledgment. Acknowledgment is made to the Donors of the American Chemical Society Petroleum Research Fund for support of this research. This research was performed in part using the Molecular Science Computing Facility (MSCF) in the William R. Wiley Environmental Molecular Sciences Laboratory, a national scientific user facility sponsored by the U.S. Department of Energy's Office of Biological and Environmental Research and located at the Pacific Northwest National Laboratory. Pacific Northwest is operated for the Department of Energy by Battelle.

IC061701L

(54) The natural electron configurations are H $1s^{0.87}$, C $2s^{1.55}2p^{2.97}$, Zr $5s^{0.16}$-$4d^{1.46}$, F $2s^{1.95}2p^{5.70}$, and H $1s^{0.87}$, C $2s^{1.55}2p^{3.02}$, Hf $5s^{0.20}4d^{1.28}$, F $2s^{1.95}$-$2p^{5.72}$ also show less involvement of Hf than Zr in the π-bonding interaction.

(55) Lyon, J. T.; Andrews, L. *Inorg. Chem.* **2006**, *45*, 9858 ($Ti + CF_4$).